A proposal of a proxy to represent an irregularity of sediment interfaces using mobile microtremor measurements

K. Motoki[(1)], T. Watanabe[(2)], K. Kato[(3)], K. Takesue[(4)], H. Yamanaka[(5)], M. Iiba[(6)], and S. Koyama[(7)]

[(1)] *Assistant General Manager, Kobori Research Complex, kmoto@kobori-takken.co.jp*
[(2)] *Manager, Kobori Research Complex, watanabe@kobori-takken.co.jp*
[(3)] *Senior General Manager, Kobori Research Complex, katokenichi@kobori-takken.co.jp*
[(4)] *Senior Manager, Kajima Corporation, k-takesue@kajima.com*
[(5)] *Professor, Tokyo Institute of Technology, yamanaka@depe.titech.ac.jp*
[(6)] *Professor, Hokkaido University, iiba-m@eng.hokudai.ac.jp*
[(7)] *Research Coordinator for Quality Control of Building, National Institute for Land and Infrastructure Management, MLIT, koyama-s92hs@nilim.go.jp*

Abstract

The subject of this article is to see if a spatial variation of horizontal to vertical spectral ratios (HVSRs) of microtremors can be regarded as a proxy of an irregularity effect of sediment-basement interface in order to readily discriminate a flat layer site from an irregular layer site. We performed 3 investigations: 1) we evaluated coefficients of variation (CVs) of HVSRs' peak periods at 4 sites based on densely mobile microtremor measurements, 2) evaluated sensitivity for CVs by numerical simulations for wave propagation with complex media, and 3) compared power spectral density estimated from CVs with that calculated from subsurface structure model. We found that CVs were 1) obviously different between flat layer sites and irregular layer sites in observed microtremors, and 2) sensitive to the slope angle of sediment interfaces. We also found that 3) CVs were related to the irregularity of the basement interfaces. As a result, we propose that CVs of 0.1 is a threshold to sort out flat layer sites where amplification factor can be approximately calculated assuming stratified media.

Keywords: microtremors, H/V spectral ratio, peak period, coefficient of variation, power spectral density

1. Introduction

An irregularly layered subsurface structure amplifies earthquake motions sometimes more than a stratified media due to, for example, a focusing effect of seismic waves [1, 2]. A depth distribution of structural boundaries can be evaluated using a drilling method[3], a surface wave exploration[4] or a successive microtremor array exploration[5]. Since these explorations are too costly for every site in practice, a preliminary examination using an easy measurement is desirable to judge whether a detail exploration is required or not.

We picked up horizontal to vertical spectral ratios (hereafter HVSRs) of microtremors as a low cost measurement. Previous researches said that amplitudes of HVSR along the fault parallel is higher than that along the perpendicular direction on the hanging wall [6, 7]. This characteristic was investigated only above relatively simple shape of boundaries, but a characteristic above complicated shape of boundaries has been not reported yet.

When HVSRs showed structural information just below a measurement point, a spatial variation of HVSRs was able to represent a spatial variation of sediment boundaries. Uebayashi *et al*. (2009) said that a HVSR technique had robustness even at a site where subsurface structure irregularly layered (hereafter an irregular layer site) [8]. On the contrary, Arai and Uebayashi (2013) reported that inverted basement depths had significant errors near basin edge and steeply changing basement-sediment interface [9]. Nakagawa and Nakai (2010) revealed that body waves induced by irregular layers contaminated surface waves [10]. Even in such wavefield, HVSRs must become not uniform but dispersed spatially. Therefore, if a spatial variation of HVSRs relates to an irregularity of sediment interface, a degree of the variation will be useful to discriminate a site where subsurface structure can be assumed to stratified media (hereafter a flat layer site).

In this paper, Focusing on a spatial variation of peak periods of HVSRs, we perfomed 3 investigations: 1) we evaluated coefficents of variation (hereafter CVs) of HVSRs' peak periods at 4 sites based on densely mobile microtremor measurements, 2) evaluated sensitivity for CVs by numerical simulations for wave propagation with complex media, and 3) compared power spectral density estimated from CVs with that calculated from subsurface structure model.

2. A method to calculate CVs of peak periods of HVSRs

We focused on a spatial variation of observed peak periods of HVSRs. A schematic image of measurement points is shown in Fig. 1, and we calculated CVs at a center and surrounding points with a distance from a center between h$\pm\Delta$h.

$$CV(h) = \sqrt{\frac{1}{n_h}\sum_{j=1}^{n_h}\left(T\left(x_j\right) - \mu\right)^2}, \tag{1}$$

where n_h is the number of stations shown in Fig. 1, $T(x_j)$ is a peak period normalized by the average of peak period, and μ is a normalized average, that is, equal to 1.

For observed microtremors, we picked up only stationary segments through a procedure shown in Fig.2. We discarded high amplitude parts exceeding a noise threshold which is set to be 3.5 times an average envelop and divided the rest into segments. We regarded HVSRs averaged for all segments as observed HVSRs. For a calculation of each spectrum, we used a logarithmic window smoothness proposed by Konno and Ohmachi (1997)[11]. Every measurement was recorded equal to and longer than 10 minutes, and more than 10 segments were picked up for each measurement. All measurements and procedures satisfied the conditions by SESAME project [12]. More detail procedure was stated in Motoki *et al*. (2016) [13].

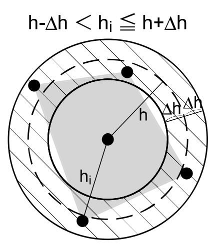

Fig. 1 – Schematic image of an area to evaluate coefficient of variation of peak periods.

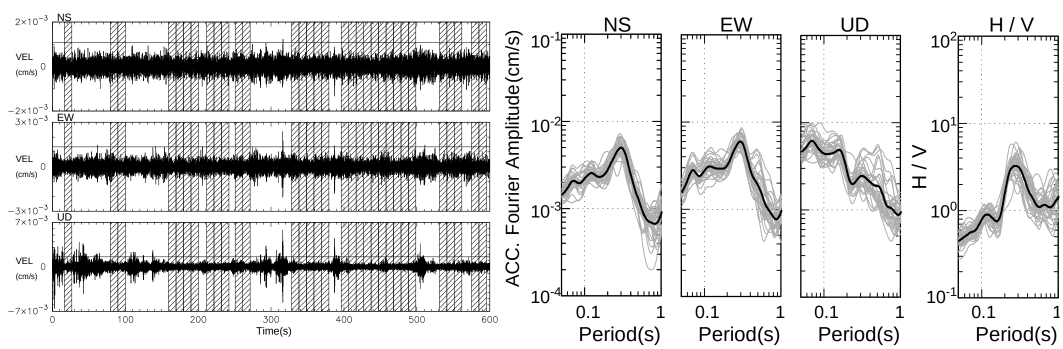

Fig. 2 – An example of waveforms, Fourier spectra and HVSR at Yamato site. Hatched segments in waveforms indicate ensembles for analysis, and gray and black lines in spectra and H/V indicate ones of each segment and average, respectively.

3. Difference of CVs between flat sites and irregular sites based on observed data

We performed densely mobile measurements at 2 irregular layer sites and 2 flat layer sites. Fig.3 shows distributions of peak periods indicated with plot sizes at Nabari site as an irregular layer site and Yamato site as a flat layer site. We also drew a distribution of depth of engineering bedrock evaluated with drilling method at Nabari site with contours and shade in Fig. 3. We arranged measurement points on the points already surveyed by a standard penetration test or a drilling method, and on the points interpolated between steeply changed depths of bedrock. We used accelerometers GPL-6A3P manufactured by Mitutoyo. All mobile measurements were conducted at daytimes on weekdays. Therefore, we considered that the surrounding sources and the characteristics of HVSRs were stable. A variation of peak periods at Nabari site shown in the left of Fig.3 was larger than that at Yamato site shown in the right of Fig. 3. At Yamato site, depths of engineering bedrock were almost constant according to results of drilling method, whereas there was some fluctuation in peak periods.

We recorded microtremors continuously for several days or more than 1 week at 4sites. For example, measurement sites at Yamato sites are shown in Fig.3. The continuous records were divided into a 10-minute long, and we evaluated a temporal variation of peak periods by calculation for each 10-minute-data as well as mobile measurement data. Transitions of peak periods of HVSR at Yamato site are shown in Fig.4. We can find that the peak periods obviously changed in a daily cycle, which means that peak periods became shorter at daytime on week days than those on weekends and at nighttime on weekdays. The temporary change implied that peak periods depended not only on subsurface structure beneath the measurement point, but also on the other effects, for example source characteristics or path characteristics. An interpretation of the fluctuation of peak period appeared in the flat layer site were discussed in Motoki *et al*.(2016) [13]. We conclude that the higher mode of Rayleigh waves and body waves were predominant near a peak period, and that not only a subsurface structure but also a distance from a source to the receiver affects a peak period.

We evaluated CVs of various interstation distances at 4 sites and plotted the average and plus-minus standard deviation of CVs in Fig.5. The interval distances were set to 10 meters at Nabari, Kakegawa and Yamato sites and to 20 meters at Tsurumi site. The black plots indicate the irregular layer sites, and the gray ones mean at the flat layer sites. We did not plot in the longer distance range than 60 meters at Kakegawa sites, because the area of Kakegawa site was relatively small and peak periods could not be found at some points where engineering bedrock was almost outcropped. A difference in the CVs between the flat layer sites and the irregular layer sites can be obviously recognized.

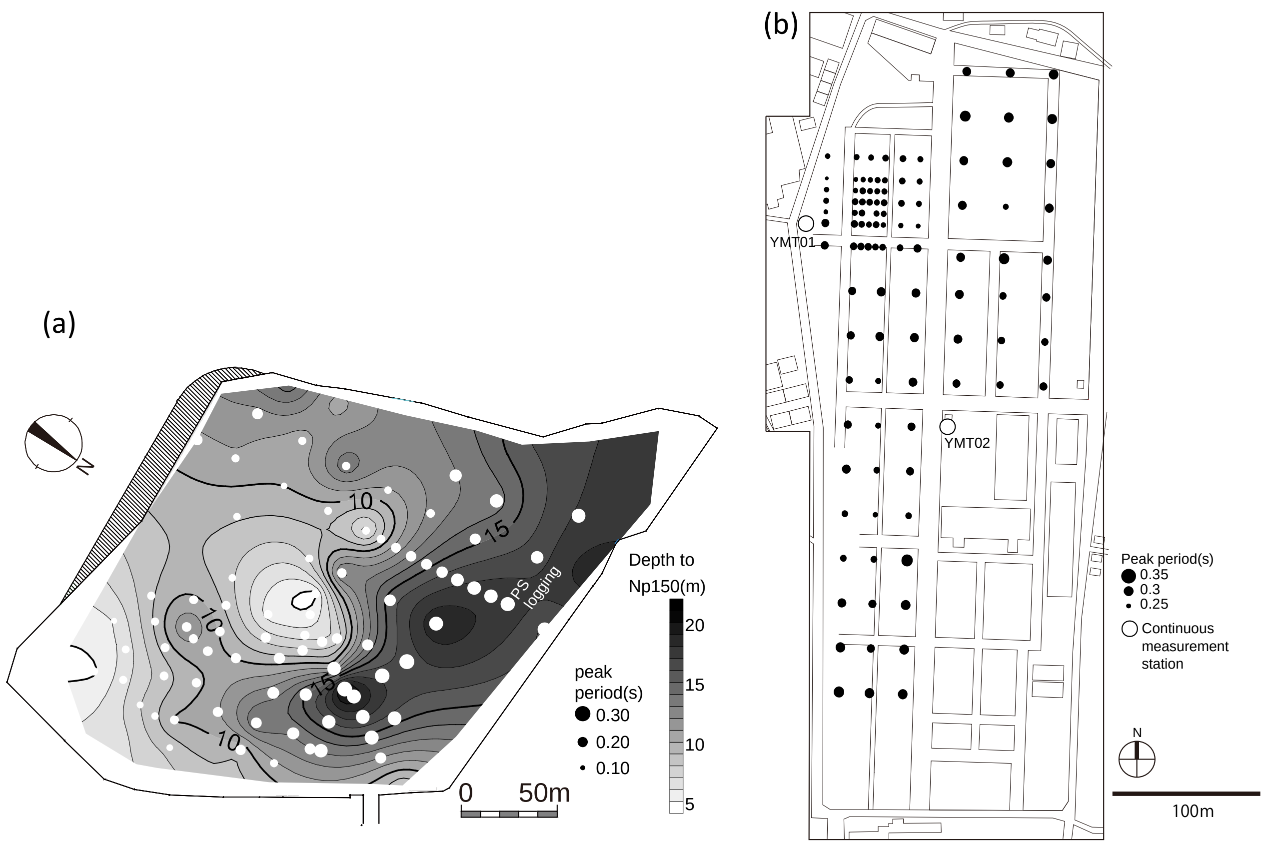

Fig. 3– (a) Distribution of peak periods of HVSR and depth of Np150 measured by drilling method [3] at Nabari site, and (b) distribution of peak periods of HVSR at Yamato site. The open circles at Yamato site indicate the continuous measurement points.

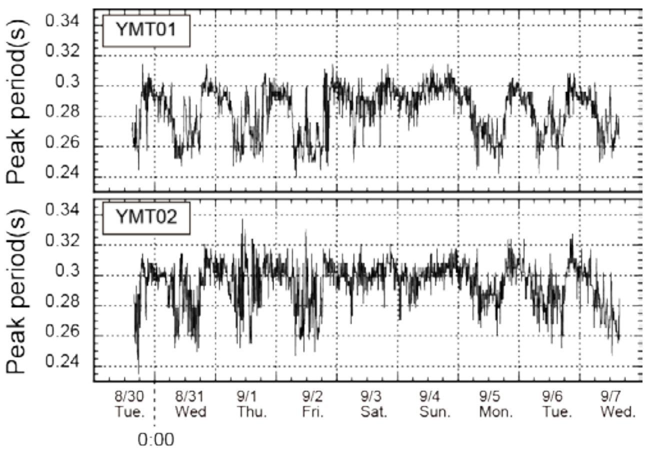

Fig. 4 – Transition of peak periods of HVSR using continuous measurements at Yamato site.

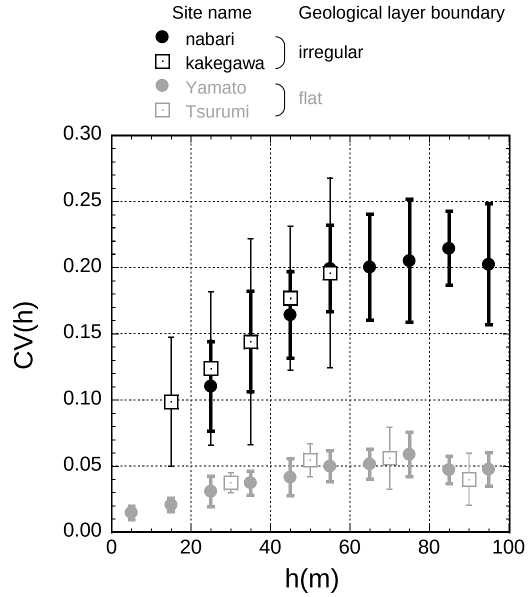

Fig. 5 – Comparison of CV of peak periods at 4 sites. The black marks indicate the results at the irregular sites, and the gray ones indicate those at the flat sites.

4. A relationship between CVs and an irregularity of sediment interfaces

We conducted numerical simulations for wave propagation with complex media in order to reveal which characteristic of shapes of sediment interfaces affected the values of CVs. After confirmation of reproducibility of the observed CVs by a simulation, we varied some parameters consisting of a subsurface structure model for a parametric study.

We selected Nabari site as a target site of numerical simulations, because peak periods could be found at all measurement points and Vs profile was already evaluated by PS logging. We used 3D FDM and constructed structure model on the basis of results of PS logging and drilling method so as to present Nabari site. We designated this model as a basic model. The physical properties are based on the result of PS logging and listed in Table 1. Although Vs of the surface layer might not be uniform, we took only irregularities of layer interfaces into account in this article. The distribution of interface depths between first and second layer and that between second layer and third layer could be estimated on the basis of results of drilling method, and interpolated using Kriging method [14], whereas the distribution of interface between third and fourth layer (hereafter the bottom interface) could not be inferred because of no information except for a PS logging point. Therefore we set 2 kinds of models for the bottom interface. One is that the thickness of third layer is constant, which is Model A in Table 2 (the basic model), and the other is that the bottom interface is flat, which is Model B in Table 2.

We deformed the basic model varying slope angle, model size and physical property of the bottom layer for a parametric study and prepared models are shown in Table 2 including Model A and B. We changed slope angles to flat, a half and 1.5 times of the basic model for Model C, D and E respectively, keeping the average depths of the layer interfaces. We enlarged the basic model to 1.5 and 2 times for Model F and G respectively. We decreased Vs of the bottom layer to 800 and 1200 for Model H and I, and also Vp of the bottom layer.

We randomly distributed 25 sources to generate vertical single force in the surrounding area at the surface. The source time functions continued for 160 seconds having the same amplitude of white noise for all, and different phase spectrum at each source.

Fig. 6 shows a comparison of distributions among peak periods of observed motions and simulated motions with Model A and Tz of the subsurface structure model. To denote a period of a subsurface structure model, we adopted Tz, which was travel time of S-wave vertically propagating from the surface of ground to the bottom interface proposed by Satoh *et al.*(2014) [15]. By and large, these distributions had similar characteristics that the north area was longer than the south area, and that the valleys of periods were evaluated in similar area drown with white arrows shown in Fig. 6. However, there were some discrepancies, for example, in the ridge shape near the broken circles shown in Fig. 6

We evaluated CVs of simulated motions as well as the observed motions shown in Fig. 7 and showed a comparison of CVs among observed motions and simulated motions with Model A and B. A characteristic of CVs that increased up to 60 meters and the inclination of CVs dropped around 60 meters were found CVs simulated with Model A and observed. However there were some discrepancy in the amplitudes, of which observed motions are evaluated between those of Model A and B. We considered that this discrepancy was due to assumptions in the shape of the bottom interface and uniformity of Vs of the surface layer. From a result of Fig.7, the actual shape of the bottom interface might be more analogous to Model A than Model B since observed CVs are close to that of Model A. Since CVs of Model A qualitatively reproduced observed CVs, we discussed characteristics of CVs only on the basis of results of numerical simulations in the following.

Next, we focused our attention on effective parameters to CVs through a parametric study. Fig. 8 shows CVs of simulated motions with Model A, C, D and E, which were prepared for an effect of slope angle. The results of these models obviously had the same tendency of inclination curve changed as stated above, but the amplitudes depended on the slope angle of subsurface structure model. CVs of simulated motions with Model A,

Table – 1 Soil physical propaties

Layer and Material		Vs (m/s)	Vp (m/s)	density (cm/s)	Q
1		220	1500	1.7	$10f^{1.0}$
2		360	1900	1.8	
3		460	2000	2	
4	α	2200	3300	2.3	
	β	800	2200	2.1	
	γ	1200	2600	2.2	

Table – 2 Parametric study cases of numerical simulations

model name	relative slope angle to Model A	relarive average depth of layer boundary to Model A	relative model size to Model A	material of the deepest layer listed in Table 2	note
Model A	1	1	1	α	basic model
Model B	1*	1	1	α	flat only on the deepest boundary
Model C	0	1	1	α	flat on all boundaries
Model D	0.5	1	1	α	half slop angles
Model E	1.5	1	1	α	1.5 times the slope angles
Model F	1	1.5	1.5	α	1.5 times the model size
Model G	1	2	2	α	2 times the model size
Model H	1	1	1	β	different material of the deepest layer
Model I	1	1	1	γ	different material of the deepest layer

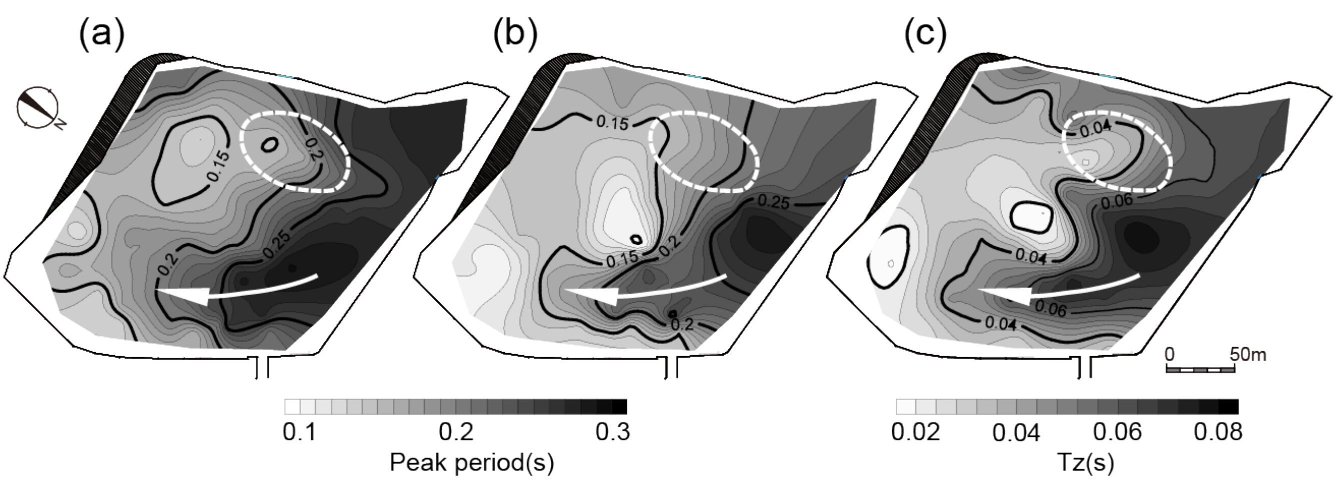

Fig. 6 – (a) Distribution of observed peak periods, (b) peak periods simulated from Model A, and (c) Tz of Model A.

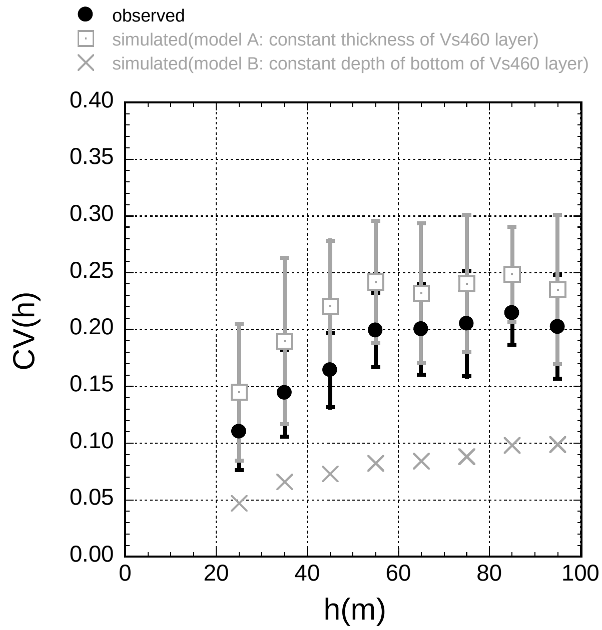

Fig. 7 –Comparison of observed and simulated CVs of peak periods. The observed one is located between the results of Model A and B, and nearer the result of Model A than that of Model B.

F and G, which have different model size from each other, are shown in Fig. 9. The lateral axis of left figure indicated an interstation distance and that of right figure indicated the distance divided by the size rate with reference to the basic model. The amplitudes of CVs were evaluated similar, and inflection distances making a smaller inclination of CVs depended on the model size. We confirmed that the impedance of soil layer did not affected the amplitude and inflection distance of CVs comparing with the other parameters, through simulations of Model H and I. We found that the amplitude of CVs were sensetive to the slope angle of subsurface structure, that the inflection distance were sensetive to the lateral size of the irregularity of interfaces. We also found that soil impedance scarcely affected CVs.

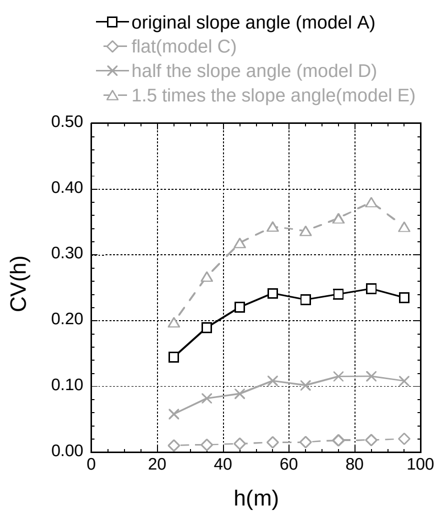

Fig. 8– Comparison of CVs simulated among models by various slope angles. These models were constructed keeping the average depths of boundaries and model sizes.

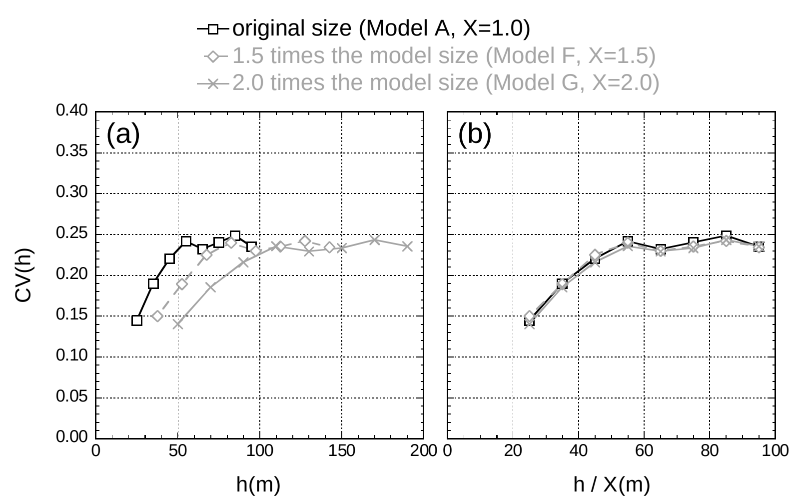

Fig. 9–Comparison of CVs simulated among models by varing model sizes. The lateral axis in (a) is set to be interstation distances and that in (b) to be the distances devided by the size rates.

To investigate a relationship between CVs of peak periods and an irregularity of subsurface structure, we made use of spectral characteristics of inhomogenieity. These characteristics are often represeted with autocorrelation function (hereafter ACF) and power spectral density function (hereafter PSDF). We compared PSDFs between a variation of peak periods and an irregurality of subsurface structures shown in Fig. 10. Before the comparison, we introduced how CVs were converted into PSDF via semivariogram. The average of CVs is expressed in the following,

$$CV(h) = \frac{1}{N}\sum_{i=1}^{N}\sqrt{\frac{1}{n_{hi}}\sum_{j=1}^{n_{hi}}\left(T\left(x_{j,i}\right)-\mu_i\right)^2}, \tag{2}$$

where N is the number of stations at which CVs were able to be calculated, i means the target station shown at the center of Fig. 1, and the other parameters are the same as equation (1). Semivariogram is expressed in the following.

$$\begin{aligned}\gamma(h) &= \frac{1}{2}\frac{1}{N_{pair}}\sum^{N_{pair}}\left(T(x+h)-T(x)\right)^2 \\ &= \frac{1}{N_{pair}}\sum^{N_{pair}}\left(T(x)-\mu\right)^2\end{aligned}, \tag{3}$$

where N_{pair} is the number of pairs whose interval distances are from h-Δh to h+Δh. Since semivariogram and CVs are dispersion and standard deviation among stations which are in limited interstation distance range, square root of semivariogram can be approximately represented to CVs.

$$\sqrt{\gamma(h)} \cong CV(h). \tag{4}$$

We confirmed that equation (4) was valid through the calculation using the result of 9 cases of the numerical simulation. Semivariogram can be expressed with autocorrelation [17],

$$\gamma(h) = \frac{1}{2}E\left[\left(T(x+h)-T(x)\right)^2\right] = R(0)-R(h), \tag{5}$$

$$R(h) = E\left[T(x+h)T(x)\right], \tag{6}$$

where E[ ] means arithmetic average, and *R(h)* means ACF. The Fourier transform of the ACF gives the PSDF as

$$P(k) = \iint R(x)e^{-ikx}dk, \tag{7}$$

$$R(x) = \frac{1}{(2\pi)^2}\iint P(k)e^{ikx}dx, \tag{8}$$

where *P(k)* is the PSDF, and k is wavenumber. Note that the PSDF can be approximately derived from CVs. In order to calculate the PSDF of peak period through an integration with equation (6), we adopted von Karman type as ACF. For 2D case, ACF can be expressed in the following [17],

$$R(x) = \frac{\varepsilon^2 2^{1-\kappa}}{\Gamma(\kappa)}\left(\frac{x}{a}\right)^{\kappa}K_{\kappa}\left(\frac{x}{a}\right), \tag{9}$$

where ε is fractional fluctuation, κ is Hurst exponent, a is a correlation distance, Γ is the gamma function, and K_κ is the modified Bessel function of the second kind of order κ. For the calculation, the source codes of these functions are quoted from SLATEC library. The appropriate ε, κ and a were searched with a grid space as L1 norm of the difference between observed and calculated CVs minimized. A comparison of CVs between observed and optimized is shown in Fig. 10. For 2D case, PSDF of von Karman type is

$$P(k) = \frac{4\pi\Gamma(\kappa+1)\varepsilon^2 a^2}{\Gamma(\kappa)\left(1+a^2k^2\right)^{\kappa+1}}. \tag{10}$$

The PSDF of peak periods can be estimated by equation (10). To compare with the PSDF derived from the peak periods, we picked up the Tz stated aboved as a parameter representing an irregularity of the subsurface structure model because a unit of parameter was adjusted to peak periods. Before calculation of the PSDF of Tz, we normalized Tz as the following equation,

$$Tz' = \frac{Tz - E[Tz]}{E[Tz]}. \tag{11}$$

A comparison between the PSDF inferred from CVs of peak periods simulated with Model A and the PSDF of Tz of Model A is shown in Fig. 12. The applicable wavelength range corresponding to interstation distances were also indicated in Fig. 12. In that range, the both PSDFs show a good agreement with each other. Comparisons of the PSDF for Model D and E, in which slope angles were changed, and for Model F and G, in which model sizes were changed, were shown in Fig. 13 as well as shown in Fig. 12. Each PSDF inferred from CVs of peak periods is consistent with the corresponding PSDF of Tz. Note that an irregularity of peak periods can be represented as an irregularity of subsurface structure.

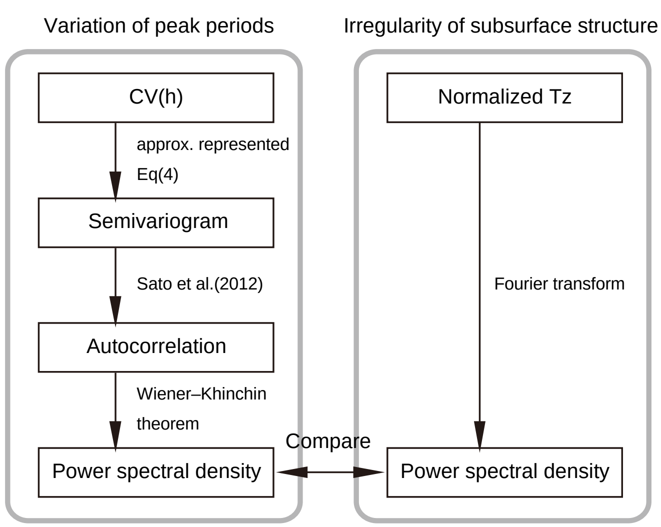

Fig. 10– Flow chart to compare a variation of peak periods directly with irregularity of subsurface structure.

5. A proposal to discriminate flat sites from irregular sites

From the results in this research and by Motoki *et al*.(2016) [13], a difference of CVs of peak periods could be imaged in Fig. 14. At a site on stratified media, amplitude of CVs must be not 0 but about 0.05. Larger CVs more than 0.05 can be represented as an irregularity of subsurface structure from an agreement of PSDF between peak periods and Tz shown in Fig. 12 and 13. CVs of peak period have possibility to discriminate a flat layer site from a irregular layer site.

In order to find an appropriate threshold of the discrimination, we made example models whose CVs at adequately long distance had 0.05, 0.10, 0.15 and 0.20. These model were assumed that there were 2 layers, the average interface depth is 20 meters, the correlation distance is 30 meters and Hurst exponent is 1.0. Vs was not required for this calculation because any Vs produced an unique result. The depth distributions of sample models whose CVs was 0.05 and 0.20 were shown in Fig. 15 (a) and (b), and the contour lines were drawn with the interval of 1 meter. The slope angles were evaluated through the least square method using the adjacent grid depth and smoothing with parzen window of band width of 40 meters which meantapproximate a half of wavelength at peak period. The probablity distributions of slope angles were shown in Fig. 15 (c). In the case

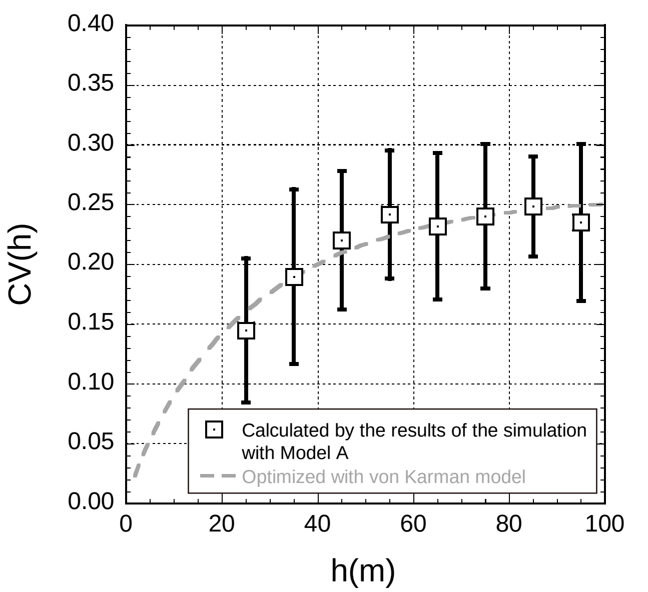

Fig. 11– CVs by simulated data from Model A, and square root of semivariogram with von Karman type of auto-correlation function using optimized parameters.

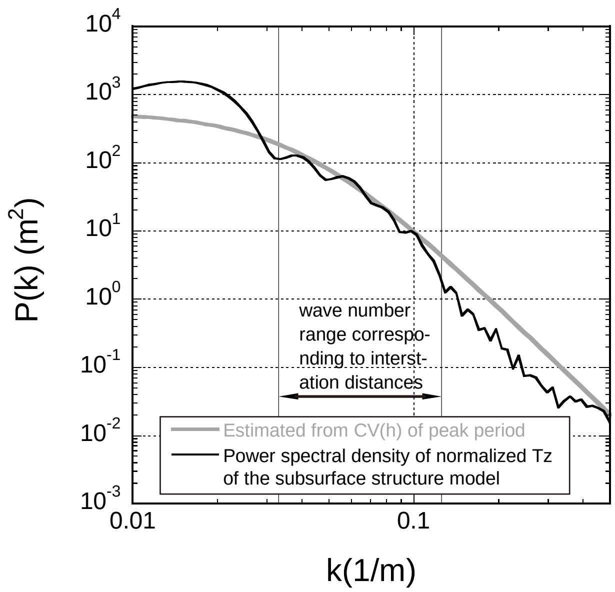

Fig. 12– Comparison of power spectral density functions between normalized Tz of Model A and estimated one by optimized parameters with CVs of peak periods.

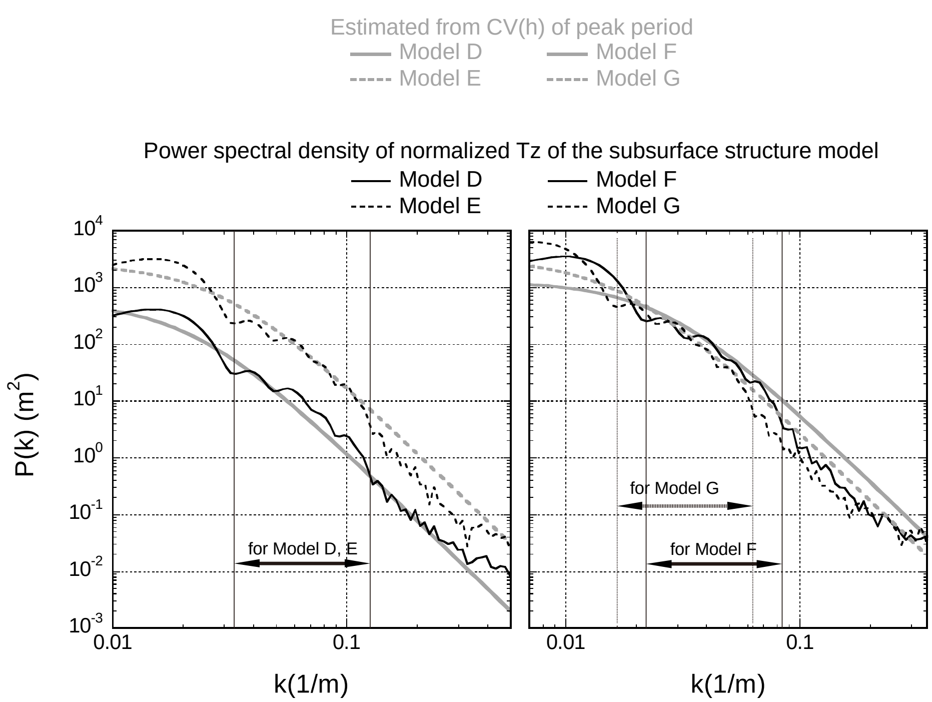

Fig. 13 – Comparison of power spectral densities between normalized Tz and estimated by CVs. Left figure shows results by various slope angles and right one does those by various model sizes.

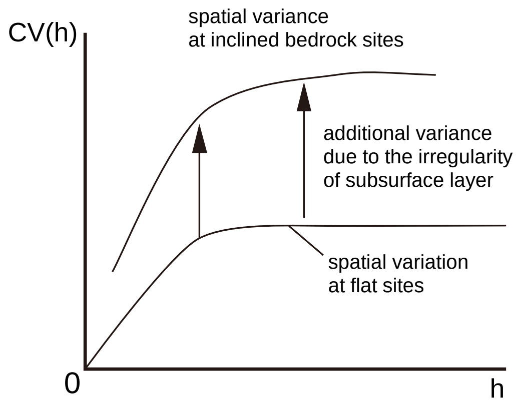

Fig. 14 – Schematic image in the difference of CVs of peak periods.

that the slope angle of layer boundary is less than 10 degree, amplification factors were little influenced by the irregulartity of layer boundary and could be approximatey estimated assuming stratified media [19]. We counted the probablity that the slope angles exceeded 10 degrees and the exceedance probabilities of each models were shown in Fig. 15 (d). It can be recognized that the probability steeply increased at CVs of 0.15. When CVs are less than 0.1, the exceedance probability can be accepted equal to 0. Therefore, a site where CVs are less than 0.1 can be regarded as a flat layer site. Although the average depth affected the probability distribution of slope angle to some extent, this threshold successfully separated in the case of an average depth of 40 meters. Consequently, we proposed a flow chart shown in Fig. 16, for an efficiently exploration of subsurface structure. It enables us to readily check if a detail exploration is required.

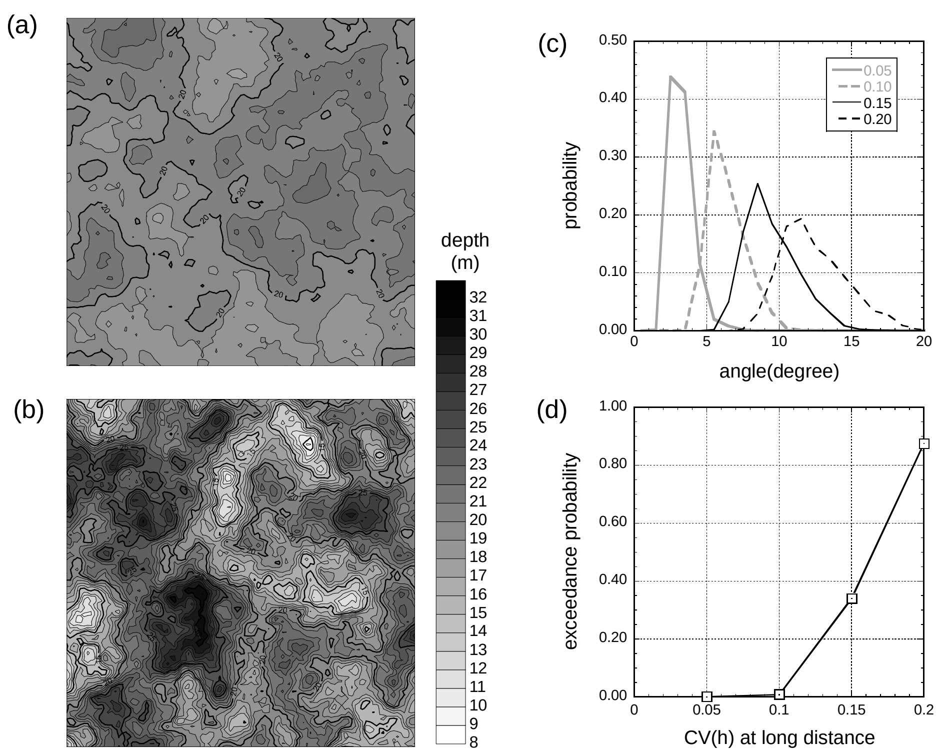

Fig. 15 – (a) Basement depth sample of CV=0.05 at a long interstation distance, (b) basement depth sample of CV=0.20, (c) probability distributions of slope angles in sample models using CVs of 0.05, 0.10, 0.15 and 0.20, and (d) exceedance probabilities that slope angles are larger than 10 degree.

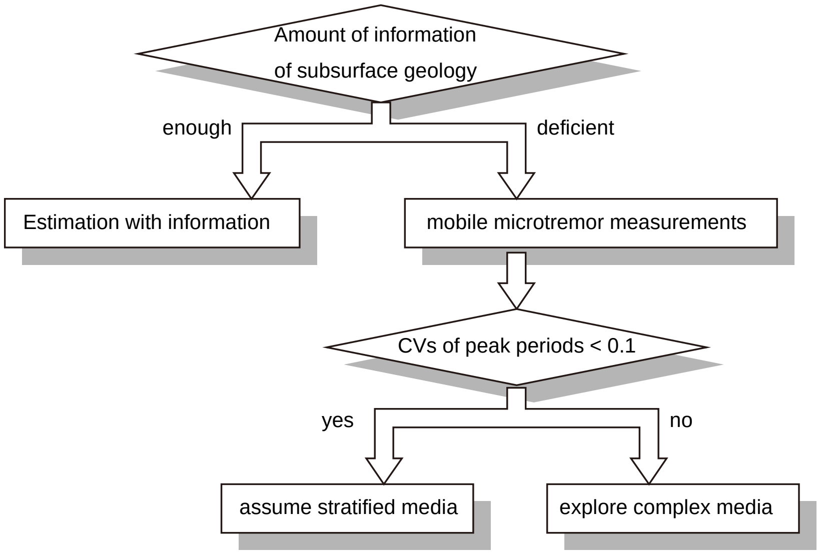

Fig. 16 – Flow chart to readily discriminate between a flat layer site and an irregular layer site.

6. Conclusions

We performed mobile microtremor measurements and numerical simulations in order to reveal that CVs of peak periods of HVSRs can be regarded as a proxy of an irregularity effect of sediment-basement interface for discrimination of a flat or irregular layer site. We concluded as follows,

1) the observed amplitudes of CVs on 2 irregular layer sites were significantly larger than those on 2 flat layer sites,

2) the simulated CVs successfully reproduced observed CVs in part, and the amplitude of CVs were affected by the slope angles of subsurface structures and the inflection distances making a smaller inclination of CVs were affected by the horizontal size of the irregularity of layer interfaces,

3) CVs can be represented as an irregularity of subsurface structure on the basis of an agreement of PSDF inferred from CVs of peak periods with PSDF calculated from Tz of subsurface structure model.

4) we proposed that a threshold of CVs was set to be 0.1 to discriminate a flat layer site from an irregular layer site.

7. Acknowledgements

We thank the late Dr. Miura for his advice and the discussions from the start time of this research. We are also grateful to Dr. Seiji Tsuno and some students of Yamanaka lab. in Tokyo Tech. for giving a hand with our microtremor measurements. Fujimori Kogyo CO., LTD. and Tyco Electronics Japan G. K. allowed us to measure microtremors at Nabari site and Kakegawa site, respectively. This research was supported in part by the fund from MLIT (Ministry of Land, Infrastructure, Transportation and Tourism, Japan).

8. References

[1] Ohori M., Koketsu K., Minami T. (1992): Seismic responses of three dimensionally sediment-filled valleys due to incident plane waves, J. Phys. Earth, Vol. 40, 209-222.

[2] Motoki K., Yamanaka H., Seo K., Kawase H. (2006): An estimation of site amplification by irregular subsurface structure near Kego fault from aftershock records of the 2005 west off Fukuoka prefecture earthquake, Journal of structural and construction engineering (Transactions of AIJ), No.602, 129-136

[3] Nishi K., Sasao H., Suzuki Y., Takesue K., Sanematsu T.(1997): A new sounding technique using rotary percussion drill, AIJ Journal of Technology and Design, No.5, 69-73.

[4] Hayashi K., Suzuki H., Saito H. (2000): Surface wave method using artificial sources –development and application to civil engineering investigations, Oyo technical report, No.21, 9-39.

[5] Motoki K., Watanabe T., Kato K., Takesue K., Yamanaka H., Iiba M., Koyama S. (2013): An evaluation of subsurface structure with inclined bedrock using microtremor array exploration, Journal of structural and construction engineering (Transactions of AIJ), Vol.78, No. 688, 1081-1088.

[6] Matsushima S., Hirokawa T., Martin F. D., Kawase H., Sánchez-Sesma F. J. (2014): The effect of lateral heterogeneity on horizontal-to-vertical spectral ratio of microtremors inferred from observation and synthetics, BSSA, Vol.104, No.1, 381-393.

[7] Uebayashi H., Kawabe H., Kamae K. (2012): Reproduction of microseism H/V spectral features using a three-dimensional complex topographical model of the sediment-bedrock interface in the Osaka sedimentary basin, Geophysical Journal International, Vol. 189, Issue 2, 1060-1074.

[8] Uebayashi H., Kawabe H., Kamae K., Miyakoshi K., Horike M. (2009): Robustness of microtremors H/V spectra in the estimation of an inclined basin-bedrock interface and improvement of the basin model in southern part in Osaka plain, Journal of structural and construction engineering (Transactions of AIJ), Vol. 74, No. 642, 1453-1460

[9] Arai H., Uebayashi H. (2013): Error of bedrock depth estimated from H/V spectrum inversion assuming flat-layered structure at a site in Osaka sedimentary basin, Summaries of technical papers of annual meeting AIJ, B-2, 207-208.

[10] Nakagawa H., Nakai S. (2010): Effect of an irregular ground on microtremor H/V spectra and dispersion curve, Journal of structural and construction engineering (Transactions of AIJ), Vol.75, No. 656, 1827-1835

[11] Konno K., Ohmachi T. (1995): A smoothing function suitable for estimation of amplification factor of the surface ground from microtremor and its application, Journal of structural mechanics and earthquake engineering, JSCE, No.525, 247-259

[12] European Commission (2005): Guidelines for the implementation of the H/V spectral ratio technique on ambient vibrations

[13] Motoki K., Watanabe T., Kato K., Takesue K., Yamanaka H., Iiba M., Koyama S. (2016): Characteristics of temporal and spatial variation in peak periods of horizontal to vertical spectral ratio of microtremors, Journal of structural and construction engineering (Transactions of AIJ), Vol.81, No. 721, 437-445

[14] Cressie N. (1993): Statistics for Spatial Data (Revised Edition)

[15] Satoh T., Okawa I., Sato T., Tohdo M., Nishikawa T. (2014): Prediction of long-period ground motions for the Nankai trough mega-earthquakes using site-specific empirical relations, Journal of structural and construction engineering (Transactions of AIJ), Vol.79, No. 695, 37-46.

[16] Davis J. C. (2002): Analysis of sequences of data, Statics and Data Analysis in Geology, 159-292

[17] Sato H., Fehler M. C., and Maeda T. (2012): 2.3.2 Mathmatical description of random media, Seismic wave propagation and scattering in the heterogeneous earth, Springer, 19-27.

[18] SLATEC Common Mathematical Library, http://www.netlib.org/slatec/

[19] Watanabe T., Kato K., Iiba M., and Koshika N. (2011): A fundamental study on effects of inclined engineering bedrock on amplification characteristics in surface layer, AIJ Journal of Technology and Design, No.36, 455-459.